MICROSTRUCTURAL CHANGES IN EXPLOSIVELY FORMED 2024-O ALUMINUM ALLOY

by

C. VENKATESH PRAKASH

B. E., University of Mysore, 1957

A MASTER'S THESIS

submitted in partial fulfillment of the

requirements for the degree

MASTER OF SCIENCE

Department of Industrial Engineering

KANSAS STATE UNIVERSITY
Manhattan, Kansas

1964

Approved by:

A E Hostetter
Major Professor

TABLE OF CONTENTS

INTRODUCTION

Principle of Explosive Forming

Explosive forming is the name given to processes which employ explosives (either high or low explosives) as the energy source for the forming of workpieces. Explosive forming is one of several high energy rate forming methods which are characterized by the suddenness of application of intense deforming loads and the brevity of their duration; that is, high energy rate forming methods shape the workpieces by applying impulsive loads. Usually, the impulsive load is applied once only, and it will be of sufficient magnitude to form the workpiece to the required shape which is fixed by a single die (male or female). The workpiece is moved through the elastic stage into the plastic stage by the impulsive force and takes a permanent set within a very short time, ranging from a few microseconds to a few milliseconds, depending on the energy source (11).

The success of explosive forming in accomplishing metal shaping is attributed to the high velocities at which the forming operations take place. High energy sources can develop forming speeds of up to 15,000 fps, as compared to 26 fps for drop hammers, and 2½ fps for drawing presses (2).

The forming velocity that can be utilized, however, depends upon the critical impact velocity or critical forming velocity of the metal being formed. At this critical velocity, the metal changes behavior from ductile to almost brittle, and its elongation drops suddenly to a negligible value (3). Each metal or

alloy seems to have its own critical forming velocity. A reduction in the order of 50 to 100 fps from the critical velocity may result in good plastic flow characteristics (12).

History

Explosives have been used for metal forming since the latter part of the nineteenth century. One of the first persons to make use of explosive forming was the American, C. E. Munroe, who in the 1880's obtained several patents to engrave, emboss, and otherwise form metals by shaped explosive charges. British and German patents were granted in the field of explosive metal forming in the 1900's. Until very recently, however, interest in this field was limited mainly to physicists, as the reaction of materials to the extremely high, yet transitory, pressures imposed on them by impulsive loading is of fundamental importance to science.

The last decade saw the advent of supersonic aircraft and missiles; conventional materials and forming methods were found to be not entirely satisfactory for their manufacture. The planes and missiles had to be fabricated from high-strength, heat-resistant materials which would retain much of their strength even at elevated temperatures. Other requirements were close tolerances and low volume production of large parts. All these created problems in forming operations, due to the lack of fabrication capabilities. In an effort to overcome the above difficulties, explosive forming was investigated, and it was found satisfactory for many production applications.

Literature Survey

One of the first companies to investigate high energy rate forming methods was the Convair Division of General Dynamics Corporation who began their experiments with a modification of the Guerin "rubber forming" process. The results showed a promising trend, and as a result, Convair experimented on a laboratory scale with a drop hammer device driven by a shotgun shell without shot. It was found that the method had the advantages of smaller production equipment, and increased ability to form parts out of high-strength materials, as compared to conventional forming methods (7).

Cartridge gases have been used in conjunction with confined fluids to form sheet metal parts. The fluid, which may be oil or water, transmits the energy of the expanding gases to the workpiece, forming the latter to the shape of the die (12). A combination of a cartridge, piston, and hydraulic fluid has also been used.

Lockheed Aircraft Corporation, of Burbank, California, used gun powder as the energy source to produce coupons for metallurgical tests in internal and external tensile testers (8).

Cartridge gases have been utilized for operations such as bulge forming and extruding, in addition to forming with dies. Convair has used gases to drive two dies into opposite sides of a blank in one operation, and the well-known "Ramset" gun uses cartridges to drive studs and other types of fasteners into metal disks.

Much work has been done on explosive forming; but the deformation mechanism of metals, under high energy rate forming methods, has not yet been clearly understood.

The most popular source of energy for explosive forming has been high explosives. Low explosives, like smokeless gun powder and black gun powder, can develop pressures in excess of 50,000 psi under sufficiently confined conditions. While this pressure is adequate for many metal forming operations, the cost of tooling is, usually, prohibitive (8).

High explosives can deliver maximum pressures of up to 4,000,000 psi, at detonation velocities of up to 28,000 fps, depending on the type of explosive. Confinement of high explosives is neither necessary nor practicable, because of the magnitude of the pressures generated. Even without confinement, the workpiece may rupture if parameters, such as weight and shape of the explosive charge, stand-off distance, and transfer medium, are not properly adjusted.

Tardif (9) formed copper cones using high explosives and found that, "Cones can be formed without danger of rupture by recessing the flat workpiece in the die cavity rather than over it"; that is, without using a blank holder to hold the blank over the die. Graphs of hardness and deformation, adapted from Tardif's paper, are shown in Fig. 1. It can be observed that in the region of the apex of the cone, the hardness values increase rather abnormally over that of the nearby portions.

It is well known that cold working increases the hardness of most metals and alloys. Similarly, explosively formed metals and

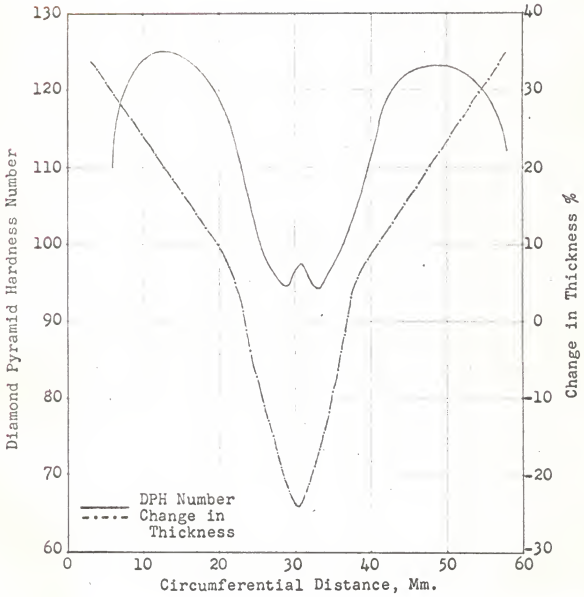

Fig. 1. Graphs of DPH number versus circumferential distance, and change in thickness per cent versus circumferential distance obtained by Tardif (9) from explosively formed copper cones.

alloys, also experience a gain in hardness. Comparison of the increased hardnesses of any metal or alloy, deformed by explosive forming and cold working, was not found during the literature survey. A comparison of the effects on the microstructure of any given metal or alloy, due to explosive forming and cold working, was also unavailable in literature.

Purpose

The objectives of the research were the following:

1. To explosively form 2024-0 aluminum alloy blanks employing Tardif's method of a recessed die, without a blank holder, and using smokeless gun powder as the energy source.

2. To determine the effects on the microstructure of the alloy, due to the forming operation.

3. To determine the effect on the hardness of the alloy, at positions deformed by various amounts during explosive forming.

4. To compare the hardness and microstructure of the explosively formed alloy with the hardness and microstructure of the same alloy, deformed by cold working to different percentages.

5. To determine whether the hardness pattern at the apex of the cones, obtained by explosively forming the aluminum alloy blanks, would follow the hardness pattern obtained by Tardif from explosively formed copper cones.

EQUIPMENT AND MATERIALS USED

Equipment

Cross sectional views of the die assembly and the firing mechanism are shown in Figs. 2 and 3, respectively.

The equipment consisted of the following parts: the forming die (Fig. 4), the die cover (Fig. 5), four spacers (Fig. 5), the cartridge holder (Fig. 5), the cover plate (Figs. 6 and 7), nuts to fasten it in position, and the firing mechanism (Fig. 3).

The forming die and die cover were machined from five-inch diameter, cold rolled, free machining, mild steel bar. The spacers and cartridge holder were machined from four-inch diameter, cold rolled, free machining, mild steel bar.

The Forming Die. The die cavity and the recess for seating the workpiece were turned in this piece. The recess for seating the workpiece was machined one-half inch deep to provide space for a blank holder, in case the apparatus did not work satisfactorily without a blank holder. A one-quarter inch diameter hole was drilled from the apex of the die cavity, through the bottom of the forming die, to vent the air during the forming cycle. A steel pipe, one-quarter inch wall thickness and five inches internal diameter, was welded to the forming die. This was to serve as a shield in case of failure of the equipment and to facilitate the welding on of the threaded rods, by means of which the cover plate would be fastened in position.

The Die Cover. The lower portion of this part was made divergent in order to spread out the pressure of the cartridge

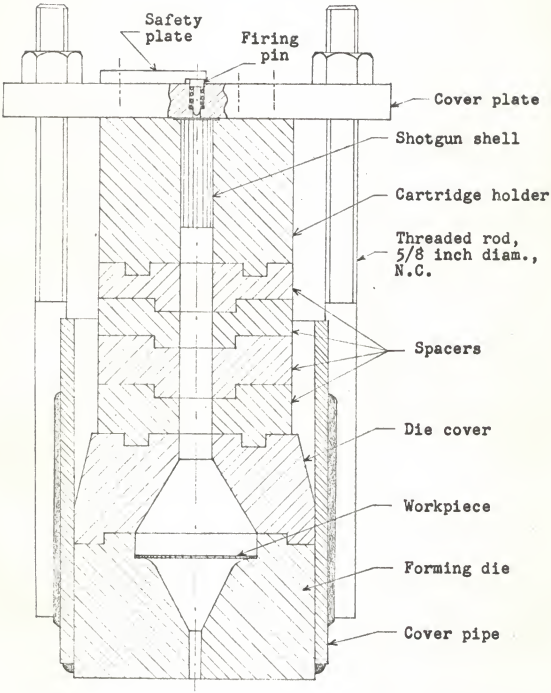

Fig. 2. Die assembly (half size).

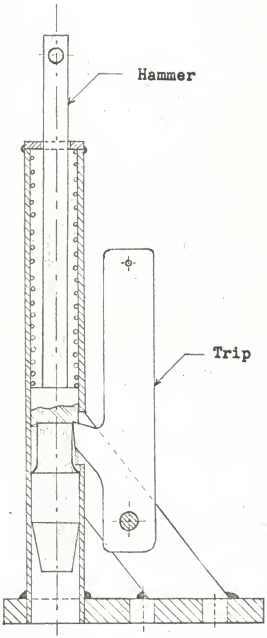

Fig. 3. Firing mechanism (full size).

gases uniformly over the entire surface of the workpiece during the forming operation. Two handles, formed from one-quarter inch diameter steel rods, were welded to this piece to facilitate its assembly with the forming die.

The Spacers. The function of the spacers was to vary the distance from the bottom of the shotgun shell to the workpiece; that is, to vary the effective barrel length, and thus the gas pressure, during the forming cycle. The maximum barrel length, measured to the top of the divergent portion in the die cover, was seven inches, and the minimum barrel length, with all the spacers removed, was three and three-quarters inches.

The Cartridge Holder. A counterbored recess was made at the top of this part, such that the cartridge would be seated flush with its top surface.

All the above parts of the equipment were provided with recesses and corresponding projections to facilitate their assembly, to make them self-aligning when assembled, and to make the assembly as gastight as possible.

The Cover Plate. The cover plate was machined from three-quarters inch thick, hot rolled, medium carbon steel plate. It was fastened in position by means of fifteen nuts and held the entire assembly together. In the center of the cover plate, a counterbored hole was drilled in which the spring loaded firing pin was placed.

The Firing Mechanism. This device consisted of a spring loaded hammer and a trip by means of which the hammer could be cocked and released. A safety plate was provided between the

Fig. 4. The forming die to which a cover pipe has been welded. Fifteen threaded rods were welded to the cover pipe for fastening the cover plate.

Fig. 5. Some parts of the equipment.

Back row, left - die cover.
Back row, right - cartridge holder.
Front row - four spacers.

hammer and firing pin (Fig. 6). The shell could be fired only when the safety plate was swung out of position (Fig. 7). The safety plate and firing mechanism were fastened to the top of the cover plate by machine screws.

The firing pin, hammer, and trip were heat treated so as to obtain a Rockwell C hardness number of 45.

Materials Used

Workpieces. The workpieces were 2.56 inches in diameter, clad 2024-0 aluminum alloy disks, punched out of 0.051 inch thick sheet. The parent metal in the "as received" condition appeared to be in the -T4 temper condition. As this was not a suitable temper for forming the alloy, all the workpieces were annealed to the -0 temper before forming, but after they were punched out.

Buffers. The buffers consisted of rubber stoppers. Initially, the rubber buffers were used without metal plugs, and later, metal plugs were used in addition.

The Shotgun Shells. Twenty gauge Western Xpert paper shot shells, of the low brass high base type, were used throughout the research. The shells were purchased, loaded only with primers. The primed shells were handloaded with powder, lead shot, and filler wads as required. When fired shells were reloaded, "Western 209 non-corrosive" primers were utilized.

Filler Wads. Twenty gauge Winchester Western nitro wads, 0.135 inch thick or 0.075 inch thick, were used for over-powder cards.

Fig. 6. The cover plate with the firing mechanism fastened to it. The hammer is in uncocked position, and the safety plate is in "safety" position.

Fig. 7. The cover plate with the firing device. The hammer is in cocked position, and the safety plate has been swung out of "safety" position. The hammer is released by pulling the trip to the right.

Twelve gauge nitro wads, 0.25 inch thick or 0.20 inch thick, and fiber wads, 0.50 inch thick, were used for pressing into the barrel portion of the equipment.

Smokeless Gun Powder. The following smokeless powders were used in this research: Alcan AL-5, AL-7, AL-8, Hercules Red Dot, and Number 2400 rifle powder.

Lead Shot. Number 8 lead shot was used throughout the research.

Lubricant. A thin layer of paraffin or grease was placed on the lower face of the blank for lubrication of the die.

PROCEDURE

Forming Technique Development

The apparatus, after preparation and assembly, was test fired with only a primed shell (no powder or shot); whereby it was found that the shell would fire only in certain positions of the spacers and die cover. This was due to a slight misalignment, in other positions, of the primer of the shell with respect to the firing pin. One of the positions in which the shell would fire was indicated by marking ink and punch marks, and the equipment was, thereafter, assembled only in the indicated position. There was no further trouble due to misfiring, when the equipment was assembled in the marked manner.

Next, a successful method for forming the blanks had to be determined, so that consistent results would be obtained.

The shotgun shells used were handloaded by means of a

"Hollywood" powder measure, a "Redding" powder scale, and a "Texan" hand reloader. The procedure adapted for handloading the shells was as set forth in the "Ideal" hand reloader's handbook. The type of powder, the weight of powder, and the weight of lead shot to make up a loaded cartridge could be varied as desired by adapting handloading. The best load of each was arrived at by trial and error.

It was thought at first that the blanks would be formed by gas pressure only. Therefore, some shots (Nos. 1 to 5, Table 1) were tried with shells loaded with powder but without any lead shot. A powder charge weighing five grains was tried in the beginning. This weight of powder was found to burn completely without leaving any residue on the workpiece after explosion. However, the pressure generated by this weight of powder was low, as attested by the barely perceptible deformation of the workpiece. When greater powder charges were used, unburned powder was invariably found on the workpiece which remained almost unformed as before.

It was conjectured that the powder was not deflagrating completely because of the loss of pressure when the gases entered the divergent portion of the die cover. Some shots (Nos. 6 to 11, Table 1) were, therefore, tried after pouring a measured volume of water into the assembly above the blank, and approximately up to the level of the cylindrical portion of the hole in the die cover. It was expected that this procedure would reduce the volume available for the gases and, hence, produce greater pressure. Also, it was expected that water would act as an at-

Fig. 8. The apparatus assembled and ready for a "shot".

Fig. 9. Materials used as buffers.

Left and right, rear - rubber stoppers.
Center - Styrofoam plug.
Front - metal plugs.

tenuating and transfer medium for the gas pressure, thus resulting in better forming of the workpieces. This improvision did not yield a better formed workpiece; also, the water made cleaning of the equipment after each shot very laborious. Hence, shots with water inside the equipment were discontinued after the 16th shot.

Another method by which greater pressure was sought was by forcing 12 gauge shotgun filler wads into the barrel, immediately in front of the cartridge, before each shot. One, one-quarter inch thick or 0.135 inch thick nitro wad was forced into the cartridge holder, and two such wads with a one-half inch thick fiber wad between them were forced into the first spacer below the cartridge holder. This innovation was used from the 6th shot onwards; but it did not yield any better results when adapted for forming operations without lead shot in the shells.

Thus, attempts to form the workpieces by gas pressure only were unsuccessful. Therefore, the shells were loaded with powder and lead shot from the 12th shot onwards. Now, however, some sort of buffer had to be used between the shell and the workpiece; otherwise the lead shot would perforate the workpiece and also mar the surface of the die cavity. The function of the buffer was to absorb the energy from the shot and wads and then transfer this energy to the workpiece. The use of buffer material would increase the load release time or pulse duration (11), but this had become unavoidable.

Rubber stoppers were used as buffers from the 12th shot for all following shots. Various configurations of buffers were

developed (Fig. 10), by gluing the stoppers together.

The shells, on being loaded with lead shot in addition to powder, went off with a sharp report on firing, in contrast to the previous cases when there was only a barely audible hissing sound.

A styrofoam plug, approximately two and three fourths inches in diameter and five-eighths inch thick (Fig. 9), was pressed into the cylindrical recess in the forming die on top of the workpiece. This was done in order to minimize the localized thinning of the workpiece, at its center, during forming (5). This procedure was adapted from the 14th shot onwards for all shots.

Several shots were fired using the above innovations, in an effort to find the weights of powder and lead shot that would give consistent results. Buffers made of rubber only proved to be unsatisfactory, as often they would be ruptured by the shot. Therefore, from the 29th shot, metal plugs were used in conjunction with the rubber buffers (Figs. 9 and 10). The type of buffer shown in Fig. 10f gave the most consistent results.

It was found, after some trials with various types of powders, that "Hercules Red Dot" smokeless powder was the most suitable, as it yielded satisfactory and consistent results even with a moderate weight of seventeen grains. The other powders tried gave equal results only with heavier weights of twenty-five to thirty grains. Therefore, "Hercules Red Dot" powder was used mostly for the forming operation, after a satisfactory forming technique had been developed.

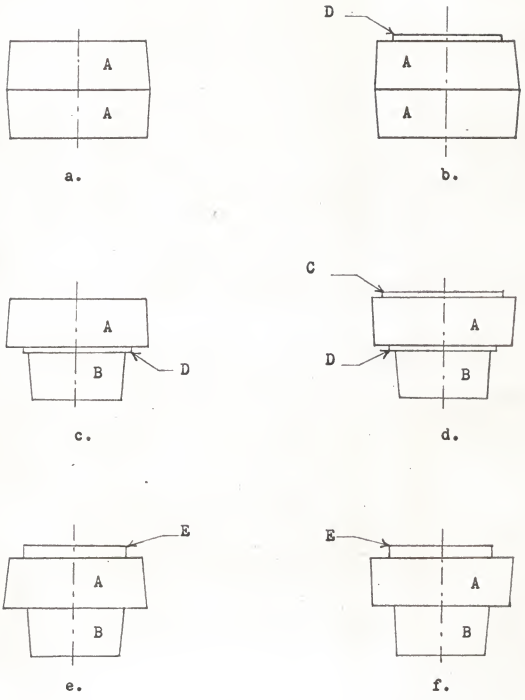

Fig. 10. Types of buffers used (full size).

A and B - rubber stoppers.
C and D - 2024-T4 aluminum plugs.
E - mild steel plug.

Details of Forming Trials

The details of the shots are shown in Table 1.

The following abbreviations have been used in Table 1: HRD, Hercules Red Dot powder; NFF, not fully formed; R, ruptured; WF, well formed; a, b, c, d, e, and f--these are the types of buffer configurations shown in Fig. 10. Unless otherwise stated, the shells were unused ones.

Study of the Deformation, Microstructure, and Microhardness of the Formed Pieces

All the well-formed pieces were in the shape of a blunt hollow cone with a wrinkled flange at its base or open end. Five specimens, namely, those obtained from shots No. 47, 50, 53, 60, and 65, were selected from the well-formed cones having approximately the same dimensions. These cones were designated as samples No. 1, 2, 3, 4, and 5, respectively, and their deformation, microstructure, and microhardness (DPH) were studied in the following manner. The average profile and dimensions of these samples were as shown in Fig. 13. The formed pieces were highly wrinkled at their base portions. In many cases the sheet metal had doubled up in one or two places, and in a few cases the doubled up portion had again been folded over, testifying to the intensity of the forming pulse.

As the deformation, microstructure and hardness would all be appreciably affected by the wrinkling and bending, the wrinkled flange portion at the base of the cone was eliminated from the subsequent studies. Only the portion that was free of bends and

Table 1. Details and results of forming trials.

Shot No.	Type of powder	Weight of powder, grains	Weight of lead shot, grains	Type of buffer	Result	Max. diam., inches	Max. depth, inches	Remarks
1	AL-5	5	0	Nil	NFF	-	-	Powder completely burned
2	AL-5	10	0	Nil	NFF	-	-	Powder incompletely burned
3	HRD	10	0	Nil	NFF	-	-	Powder incompletely burned
4	AL-8	10	0	Nil	NFF	-	-	Powder incompletely burned
5	AL-7	10	0	Nil	NFF	-	-	Powder incompletely burned
6	AL-5	5	0	Water only	NFF	-	-	Powder completely burned
7	AL-5	20	0	Water only	NFF	-	-	Powder incompletely burned
8	AL-5	10	0	Water only	NFF	-	--	Powder incompletely burned
9	HRD	15	0	Water only	NFF	-	-	Powder incompletely burned
10	#2400 Rifle powder	5	0	Water only	NFF	-	--	Some powder residue seen

Table 1 (Cont.).

Shot No.	Type of powder	Weight of powder, grains	Weight of lead shot, grains	Type of buffer	Result	Max. diam., inches	Max. depth, inches	Remarks
11	AL-5	15	Nil	Water only	NFF	-	-	Powder incompletely burned
12	HRD	20	110	a + 60ml. of water	NFF	-	-	Powder completely burned
13	HRD	25	110	a + 40ml. of water	R	-	-	
14	HRD	20	110	a + 50 ml. of water	NFF	-	-	Reloaded cartridge
15	HRD	25	110	a + 50ml. of water	R	-	-	Reloaded cartridge
16	HRD	23	110	a + 40ml. of water	WF	2 1/16	1 1/8	Reloaded cartridge
17	HRD	23	110	a	R	-	-	Reloaded cartridge
18	HRD	20	110	a	NFF	-	-	Reloaded cartridge
19	HRD	21	110	a	NFF	-	-	Reloaded cartridge
20	HRD	22	110	a	NFF	-	-	Reloaded cartridge
21	HRD	22	110	a	R	-	-	
22	HRD	20	110	a	NFF	-	-	
23	HRD	21	110	a	NFF	-	-	
24	HRD	21½	110	a	WF	2 1/32	1 3/16	
25	HRD	22½	110	a	NFF	-	-	Reloaded cartridge
26	HRD	22	110	a	R	-	-	

Table 1 (Cont.).

Shot No.	Type of powder	Weight of powder, grains	Weight of lead shot, grains	Type of buffer	Result	Max. diam., inches	Max. depth, inches	Remarks
27	HRD	21	150	a	R	-	-	
28	HRD	20	150	a	NFF	-	-	Reloaded cartridge
29	HRD	20	150	b	NFF	-	-	
30	HRD	22	150	b	R	-	-	
31	HRD	21	150	b	WF	2 1/16	1 1/16	
32	HRD	20	150	c	R	-	-	
33	HRD	18	150	c	NFF	-	-	
34	HRD	19	150	c	R	-	-	
35	HRD	19	150	d	R	-	-	
36	HRD	19	110	d	R	-	-	
37	HRD	18	110	d	WF	-	-	Eccentrically formed
38	HRD	18	150	d	WF	2 1/16	1 1/8	
39	HRD	22	150	e	R	-	-	
40	HRD	20	150	e	R	-	-	
41	HRD	19	150	e	WF	2	1 3/16	
42	HRD	19	200	e	R	-	-	
43	HRD	18	200	e	WF	2 1/16	1 1/8	
44	HRD	19	200	f	R	-	-	
45	HRD	18	200	f	R	-	-	
46	HRD	16	200	f	NFF	-	-	
47	HRD	17	200	f	WF	2	1 3/16	
48	HRD	17½	200	f	R	-	-	
49	HRD	17	200	f	WF	2 1/16	1 1/8	
50	HRD	17	200	f	WF	2	1 3/16	
51	HRD	17	200	f	WF	2 1/16	1 1/16	
52	HRD	17	200	f	WF	2	1 1/4	

Table 1 (concl.).

Shot No.	Type of powder	Weight of powder, grains	Weight of lead shot, grains	Type of buffer	Result	Max. diam., inches	Max. depth, inches	Remarks
53	HRD	17	200	f	WF	2	1 3/16	
54	AL-5	20	150	f	NFF	-	-	
55	AL-5	20	200	f	NFF	-	-	
56	AL-5	22	200	f	NFF	-	-	
57	AL-5	25	200	f	WF	2 1/16	1 1/16	
58	AL-7	20	200	f	NFF			
59	AL-8	22	200	f	NFF			
60	HRD	17	200	f	WF	2	1 3/16	
61	HRD	17	200	f	WF	2 1/16	1 1/16	
62	HRD	17	200	f	WF	2	1 3/16	
63	HRD	17	200	f	WF	2	1 3/16	
64	HRD	17	200	f	WF	-	-	Eccentrically formed
65	HRD	17	200	f	WF	2	1 3/16	
66	HRD	17	200	f	WF	2	1 3/16	

wrinkles, that is, the portion of the formed pieces that had actually been shaped to the configuration of the die cavity, was further examined and studied. This was the portion marked 1, 2, . . . 22, 23 in Fig. 13, and was obtained by stepping off with a pair of dividers, eleven one-eighth inch divisions on either side of the apex of the cone.

Mounting of the Specimens. The sample cones selected for further study were cut into two symmetrical halves on a band saw. From one of these halves of each sample a V-shaped strip approximately one-fourth inch wide was cut (Fig. 12), the new cut being parallel to the first cut. This strip was then cut into pieces of about half an inch length for mounting. The mounting itself was done to facilitate subsequent handling of the strips. Bakelite was used as the mounting material, and care was taken that the correct side of the strip (the surface obtained by the first saw cut) was presented for examination after mounting. Some mounted samples are shown in Fig. 14. Each of the mounted specimens was identified by scribed numbers on its back face and also on its curved face.

Grinding and Polishing. The mounted samples were prepared for microscopic examination by the usual method of successively grinding and lapping with alumina abrasive of finer grit sizes. The specimens were polished on a gamal cloth covered lap, running 90 rpm, using levigated heavy magnesium oxide as the abrasive. Final polishing was done on a gamal cloth covered lap, washed clean of abrasive, and moistened slightly with distilled water. More details about grinding and polishing aluminum alloys are

Fig. 11. The workpiece (front, left) and formed pieces shaped to various amounts. The sample in the center of back row shows the maximum forming obtained without rupture of the explosively formed piece. Samples formed to a greater degree were always cracked or ruptured.

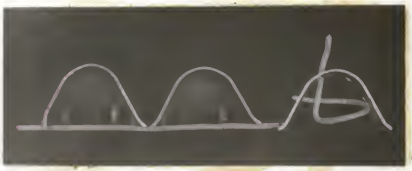

Fig. 12. The st[illegible] at right was cut out of an explosively formed sample preparatory to mounting in bakelite. The profile at the center of the formed piece is clearly seen, and also the wrinkles at the base.

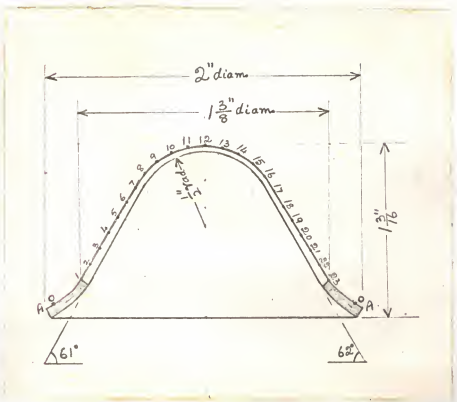

Fig. 13. Average profile of the samples studied for the amount of deformation, microstructure, and hardness. The numbers 1-23 indicate the positions at which these studies were made.

Fig. 14. Samples mounted in bakelite.

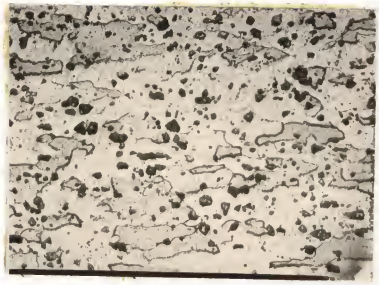

Fig. 15. Typical microstructure of the "as received" 2024 aluminum alloy sheet. The microstructure suggests the stable -T4 temper. Etched, 500 X.

found in the literature (6).

Etching the Samples. The samples were etched immediately after a polished stain-free surface was obtained. The following etchants were tried initially, in order to find the one most suitable:

1. Keller's concentrated etch diluted 9:1 by volume with distilled water.

2. Keller's concentrated etch diluted 9:2 by volume with distilled water.

3. A solution of concentrated nitric acid in distilled water, in the ratio 1:3 by volume. Etching temperature 158°-160°F.

4. A solution of the following composition: 1/2 gm. sodium fluoride, 1 ml. concentrated hydrochloric acid, 2 ml. concentrated nitric acid, 97 ml. distilled water.

The fourth etchant was found to be most suitable, and it was used throughout. The etching time varied between 15-20 seconds for the "as received" material (2024-T4), 40-50 seconds for the annealed unformed material (2024-0), and 30-40 seconds for the formed material, shorter time being required for the more deformed material. Fresh etchant was prepared each day. After etching, the samples were stored in a desiccator until required for further examination. The samples were polished and etched again, if on microscopic examination the surface was found to contain scratches.

Microstructure and Deformation. The etched specimens were studied under the microscope to investigate whether there had

been any changes in the microstructure as a result of the forming operation. The microstructures of the "as received" sheet and of the annealed unworked material are shown in Figs. 15 and 16, respectively. A Bausch and Lomb metallograph was used for photomicrography. Photomicrographs were taken at various locations on the specimens for the purposes of record and study, and some are shown in Figs. 17 and 18.

It was apparent that the samples were not of uniform thickness, showing that they had been deep drawn by various amounts at different positions. Therefore, in order to measure the pattern of these differing amounts of deformation, scribe marks were made at one-eighth inch intervals on the polished samples. These marks were then located in the field of view of the microscope, and the thickness of the sample at each position given by the scribe mark was measured with a Filar eyepiece.

Microhardness (DPH). A microhardness tester with a DPH (diamond pyramid hardness) indenter was used for studying the hardness pattern of the specimens. To find the hardness at a particular position, the scribe mark denoting the position was first located in the field of view of the microhardness tester. The width of the specimen at the required position was then measured, as a check against the width obtained by the metallograph. Then a suitable point, located approximately at the center of the width and in the vicinity of the scribe mark, was chosen for the hardness test area. The point was chosen such that it was at least two and one-half diagonal lengths (of the expected indentation) away from the edge of the scribe mark to

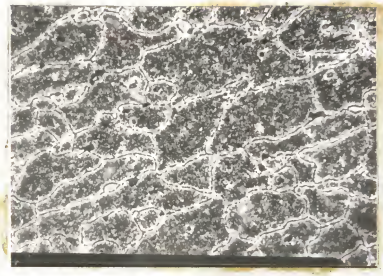

Fig. 16. Photomicrograph of 2024-O (annealed) aluminum alloy. The grains are of α solid solution (copper in aluminum). The white network along the grain boundaries is precipitated Al_2Cu. The small dark discrete spots are the insoluble compounds (Mg-Si) and (Al-Cu-Fe-Mn). Etched, 500 X.

Fig. 17. Photomicrograph of an explosively formed specimen at a section deformed approximately 25% (position 2, Table 2). The elongation and preferred orientation of the grains (compare with Fig. 16) are clearly noticeable. Etched, 500 X.

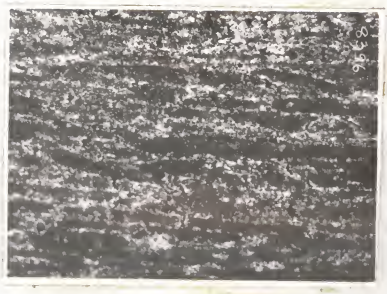

Fig. 18. Photomicrograph of an explosively formed specimen in the region of the apex (position 12, Table 4). The deformation at this position was 62.7%. Etched, 500 X.

the center of the indentation, so that the hardness value obtained would not be affected by work hardening due to the marking. After a suitable point was selected, the objective of the tester was replaced by the indenter, and the hardness measurement was made. The applied load for determining the DPH was twenty gm. throughout the course of the research work, and the duration of application of the load was seven seconds, as timed by a stop-clock. The twenty gm. load was chosen as it produced a more clearly visible indentation than a ten gm. load which was also tried initially. If, by mischance, an indentation was obtained too close to the scribe mark, the hardness corresponding to the indentation was not measured; and another test was made at a point at least two and one-half diagonal lengths away from both the scribe mark and the rejected indentation.

Two hardness tests, one on each side of the scribe mark, were made, and their average value was taken as the DPH at the position. The above procedure was adapted for all samples for all the positions. Some photomicrographs of the indented samples are shown in Figs. 19 and 20.

The observed values of the thickness and DPH for the five samples are given in Tables 2-6.

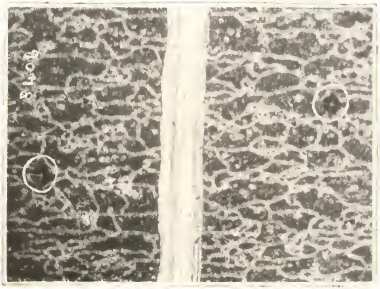

Fig. 19. DPH test indentation marks (circled) on an annealed, unformed workpiece. The average DPH number of such samples was 58.4. The white band in the center is the scribe mark. Etched, 250 X.

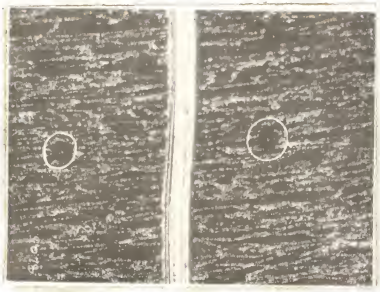

Fig. 20. DPH test indentation marks (circled) in the region of the apex of an explosively formed specimen. The average DPH number at the apex was 85.1 (position 12, Table 7). Etched, 250 X.

Table 2. Sample No. 1, cone obtained from shot No. 47 (Table 1).

Position on sample	Thickness of section, inches	Diagonal lengths as measured by microscope				Average diagonal, d, mm.	Actual length of mean diagonal d x .0154 mm.	DPH
		d_1 mm.	d_1^1 mm.	d_2 mm.	d_2^1 mm.			
1	.040	1.46	1.43	1.50	1.45	1.46	.0224	73.9
2	.038	1.62	1.58	1.50	1.45	1.54	.0237	66.0
3	.036	1.55	1.51	1.45	1.50	1.50	.0232	68.9
4	.035	1.45	1.47	1.51	1.44	1.47	.0226	72.6
5	.033	1.35	1.41	1.45	1.49	1.43	.0220	76.6
6	.031	1.39	1.44	1.34	1.36	1.38	.0213	81.8
7	.031	1.28	1.22	1.35	1.43	1.32	.0203	90.0
8	.030	1.35	1.40	1.27	1.33	1.34	.0206	87.4
9	.028	1.36	1.35	1.36	1.41	1.37	.0211	83.3
10	.026	1.38	1.35	1.36	1.44	1.38	.0213	81.8
11	.022	1.49	1.45	1.40	1.37	1.43	.0220	76.6
12	.020	1.37	1.34	1.37	1.43	1.38	.0212	82.5
13	.020	1.49	1.45	1.45	1.37	1.44	.0222	75.3
14	.021	1.36	1.40	1.40	1.49	1.41	.0218	78.0
15	.024	1.36	1.32	1.37	1.40	1.36	.0210	84.1
16	.028	1.34	1.28	1.40	1.35	1.34	.0207	86.6
17	.029	1.41	1.35	1.28	1.25	1.32	.0204	89.1
18	.030	1.40	1.49	1.32	1.37	1.40	.0215	80.2
19	.032	1.51	1.44	1.41	1.37	1.43	.0221	75.9
20	.033	1.45	1.44	1.51	1.43	1.46	.0224	73.9
21	.036	1.63	1.56	1.52	1.39	1.52	.0235	67.2
22	.038	1.62	1.55	1.51	1.44	1.53	.0236	66.6
23	.039	1.44	1.30	1.51	1.41	1.41	.0218	78.0

Table 3. Sample No. 2, cone obtained from shot No. 50 (Table 1).

Position on sample	Thickness of section, inches	Diagonal lengths as measured by microscope				Average diagonal	Actual length of mean diagonal	DPH
		d_1 mm.	d_1^1 mm.	d_2 mm.	d_2^1 mm.	d, mm.	d x .0154 mm.	
1	.041	1.37	1.41	1.45	1.40	1.43	.0220	76.6
2	.039	1.48	1.57	1.57	1.46	1.53	.0234	67.7
3	.038	1.46	1.48	1.53	1.49	1.49	.0230	70.1
4	.035	1.49	1.51	1.39	1.45	1.46	.0224	73.9
5	.034	1.50	1.40	1.34	1.43	1.42	.0218	78.0
6	.031	1.40	1.36	1.37	1.34	1.37	.0211	83.3
7	.030	1.29	1.36	1.31	1.27	1.30	.0201	91.8
8	.028	1.40	1.36	1.26	1.28	1.33	.0205	88.3
9	.028	1.35	1.41	1.36	1.31	1.36	.0209	84.9
10	.025	1.37	1.31	1.39	1.44	1.38	.0212	82.5
11	.021	1.48	1.46	1.38	1.35	1.41	.0218	78.0
12	.018	1.36	1.40	1.35	1.36	1.37	.0211	83.3
13	.020	1.37	1.45	1.42	1.47	1.43	.0220	76.6
14	.022	1.40	1.38	1.38	1.43	1.40	.0215	80.2
15	.026	1.40	1.33	1.35	1.31	1.34	.0207	86.6
16	.029	1.31	1.32	1.28	1.33	1.32	.0204	89.1
17	.029	1.40	1.36	1.28	1.22	1.31	.0202	90.9
18	.031	1.32	1.40	1.30	1.42	1.36	.0210	84.1
19	.033	1.48	1.43	1.33	1.40	1.41	.0217	78.8
20	.034	1.39	1.36	1.53	1.47	1.43	.0221	75.9
21	.037	1.51	1.57	1.43	1.48	1.50	.0231	69.5
22	.039	1.45	1.47	1.59	1.52	1.51	.0232	68.9
23	.040	1.37	1.43	1.47	1.49	1.44	.0222	75.3

Table 4. Sample No. 3, cone obtained from shot No. 53 (Table 1).

Position on sample	Thickness of section, inches	Diagonal lengths as measured by microscope				Average diagonal: d, mm.	Actual length: of mean diagonal d x .0154 mm.	DPH
		d_1 mm.	d_1^1 mm.	d_2 mm.	d_2^1 mm.			
1	.039	1.40	1.38	1.44	1.55	1.45	.0222	75.3
2	.038	1.45	1.48	1.48	1.61	1.53	.0236	66.6
3	.034	1.48	1.44	1.53	1.47	1.48	.0228	71.3
4	.034	1.39	1.41	1.51	1.45	1.44	.0222	75.3
5	.033	1.32	1.39	1.42	1.47	1.40	.0216	79.5
6	.033	1.48	1.43	1.25	1.28	1.36	.0210	84.1
7	.032	1.25	1.33	1.37	1.25	1.30	.0200	92.7
8	.029	1.39	1.35	1.29	1.25	1.32	.0204	89.1
9	.026	1.27	1.37	1.42	1.34	1.35	.0208	85.7
10	.025	1.44	1.37	1.31	1.36	1.37	.0211	83.3
11	.020	1.43	1.48	1.33	1.40	1.41	.0217	78.8
12	.019	1.24	1.29	1.49	1.42	1.36	.0210	84.1
13	.021	1.40	1.45	1.39	1.44	1.42	.0219	77.3
14	.021	1.36	1.40	1.41	1.39	1.39	.0214	81.0
15	.024	1.28	1.33	1.35	1.40	1.34	.0206	87.4
16	.028	1.34	1.27	1.28	1.35	1.31	.0202	90.9
17	.029	1.27	1.31	1.36	1.26	1.30	.0200	92.7
18	.030	1.29	1.24	1.49	1.42	1.36	.0210	84.1
19	.033	1.32	1.41	1.47	1.44	1.41	.0217	78.8
20	.035	1.51	1.41	1.37	1.43	1.43	.0220	76.6
21	.037	1.45	1.49	1.48	1.54	1.49	.0230	70.1
22	.038	1.53	1.51	1.46	1.50	1.50	.0231	69.5
23	.041	1.46	1.50	1.40	1.43	1.46	.0223	74.6

Table 5. Sample No. 4, cone obtained from shot No. 60 (Table 1).

Position on sample	Thickness of section, inches	Diagonal lengths as measured by microscope				Average diagonal	Actual length of mean diagonal	DPH
		d_1 mm.	d_1^1 mm.	d_2 mm.	d_2^1 mm.	d, mm.	d x .0154 mm.	
1	.038	1.33	1.36	1.50	1.41	1.40	.0215	80.2
2	.038	1.58	1.49	1.39	1.46	1.48	.0228	71.3
3	.037	1.37	1.47	1.53	1.42	1.45	.0223	74.6
4	.034	1.51	1.40	1.32	1.42	1.41	.0217	78.8
5	.032	1.34	1.46	1.40	1.32	1.38	.0212	82.5
6	.032	1.33	1.26	1.31	1.44	1.34	.0206	87.4
7	.030	1.15	1.24	1.33	1.37	1.27	.0196	96.5
8	.030	1.17	1.25	1.45	1.30	1.29	.0199	93.7
9	.027	1.33	1.37	1.25	1.31	1.31	.0203	90.0
10	.024	1.45	1.32	1.28	1.31	1.34	.0206	87.4
11	.021	1.44	1.37	1.39	1.32	1.38	.0212	82.5
12	.019	1.34	1.40	1.29	1.25	1.32	.0204	89.1
13	.022	1.28	1.40	1.37	1.51	1.39	.0214	81.0
14	.022	1.35	1.47	1.37	1.26	1.36	.0210	84.1
15	.025	1.42	1.32	1.33	1.20	1.32	.0204	89.1
16	.027	1.35	1.26	1.25	1.33	1.30	.0200	92.7
17	.030	1.27	1.18	1.30	1.38	1.28	.0197	95.6
18	.030	1.34	1.25	1.37	1.45	1.35	.0208	85.7
19	.032	1.41	1.30	1.48	1.39	1.39	.0214	81.0
20	.035	1.40	1.33	1.48	1.38	1.40	.0216	79.5
21	.038	1.39	1.43	1.50	1.53	1.46	.0225	73.3
22	.038	1.40	1.51	1.43	1.53	1.47	.0226	72.6
23	.039	1.42	1.38	1.42	1.30	1.38	.0212	82.5

Table 6. Sample No. 5, cone obtained from shot No. 65 (Table 1).

Position on sample	Thickness of section, inches	Diagonal lengths as measured by microscope				Average diagonal:	Actual length: of mean diagonal	DPH
		d_1 mm.	d_1^1 mm.	d_2 mm.	d_2^1 mm.	d, mm.	d x .0154 mm.	
1	.041	1.47	1.39	1.41	1.34	1.40	.0216	79.5
2	.040	1.54	1.50	1.45	1.52	1.50	.0231	69.5
3	.038	1.45	1.48	1.51	1.44	1.47	.0226	72.6
4	.037	1.36	1.40	1.45	1.51	1.43	.0220	76.6
5	.035	1.42	1.36	1.40	1.40	1.39	.0214	81.0
6	.033	1.34	1.28	1.40	1.33	1.34	.0207	86.6
7	.032	1.25	1.31	1.20	1.37	1.28	.0198	94.6
8	.031	1.28	1.35	1.25	1.31	1.30	.0201	91.8
9	.027	1.35	1.42	1.33	1.27	1.34	.0206	87.4
10	.024	1.27	1.38	1.41	1.35	1.35	.0208	85.7
11	.020	1.37	1.44	1.32	1.38	1.38	.0213	81.8
12	.019	1.42	1.32	1.27	1.35	1.34	.0207	86.6
13	.018	1.41	1.50	1.31	1.38	1.40	.0215	80.2
14	.020	1.40	1.31	1.36	1.42	1.37	.0211	83.3
15	.023	1.29	1.22	1.35	1.43	1.32	.0203	90.0
16	.028	1.35	1.30	1.32	1.24	1.30	.0201	91.8
17	.030	1.24	1.31	1.30	1.26	1.28	.0198	94.6
18	.031	1.25	1.35	1.41	1.34	1.34	.0207	86.6
19	.033	1.36	1.44	1.40	1.31	1.38	.0212	82.5
20	.033	1.43	1.31	1.39	1.47	1.40	.0215	80.2
21	.036	1.51	1.45	1.48	1.45	1.47	.0226	72.6
22	.037	1.57	1.49	1.39	1.44	1.47	.0227	72.0
23	.038	1.35	1.46	1.33	1.39	1.38	.0213	81.8

Cold Working and Study of the Cold Worked 2024-0 Aluminum Alloy

Cold Working. Strips of the alloy approximately one-fourth inch wide and two inches long were cut by means of a pair of sheet metal shears from an annealed disk of the alloy (2024-0) sheet. A two-high manually operated rolling mill was utilized to cold work the strips. The distance between the rolls was preset to deform the sheet thickness by a certain approximate amount. Then one of the strips was deformed (cold worked) by passing it through the rolls in a single continuous pass. Several strips were deformed in this way, each strip by a different amount.

Microstructure and Deformation. The cold rolled strips were mounted in bakelite and prepared for microscopic examination in a manner similar to that adapted for the explosively formed samples. Then the samples were examined in the metallograph to study their microstructure. Photomicrographs of some rolled samples are shown in Figs. 21 and 22.

The thickness of each sample was also measured at three different places on it by a Filar eyepiece, and the average value of the thickness of each specimen was obtained.

Microhardness (DPH). The hardness of each of the samples was then measured. The procedure adapted was similar to that followed for the explosively formed samples.

Photomicrographs of some indented samples are shown in Figs. 23 and 24.

Fig. 21. Photomicrograph of a cold rolled specimen deformed 43.2% (trial No. 7, Table 9). The elongation and crystallographic fibering of the grains is apparent (compare with Fig. 16). Etched, 500 X.

Fig. 22. Photomicrograph of a cold rolled specimen deformed 78.5% (trial No. 10, Table 9). The extreme fragmentation of the grains and consequent grain refinement is noticeable. Etched, 500 X.

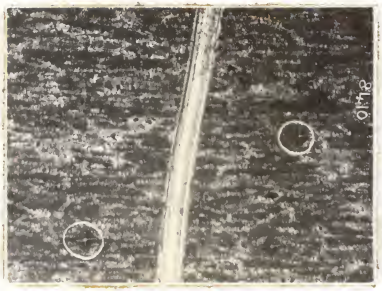

Fig. 23. DPH test indentations (circled) on a specimen deformed 43.2% by cold rolling. The DPH number obtained was 95.6 (trial No. 7, Table 9). The white band in the center is the scribe mark. Etched, 250 X.

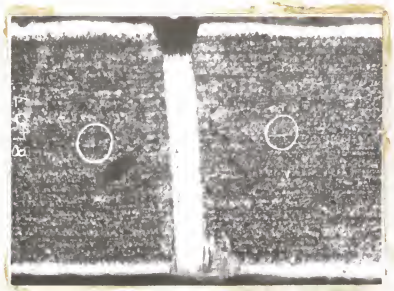

Fig. 24. DPH test indentation marks (circled) on a cold rolled specimen deformed 78.5%. The DPH measured was 104.9 (trial No. 10, Table 9). The white bands at the top and bottom are the relatively pure aluminum cladding. Etched, 250 X.

RESULTS

Explosively Formed Samples

The wrinkled portion at the base of the cones was examined, and it was found that the metal thickness varied from 0.054 inch at A to approximately 0.040 inch at 1 and 23 (Fig. 13). Since the original sheet was 0.051 inch thick, there appeared to be an increase in thickness at some positions of up to 0.003 inch, due to the forming operation. Such a phenomenon is termed as "metal gathering".

The microhardness was also measured at a number of places in this portion of wrinkling and apparent metal gathering. The DPH was found to vary from 62.3 units to 79.5 units, while the DPH of the annealed unworked sheet was 58.4. There was, thus, an increase in hardness of between 3.9 and 21.1 units in this region. Near the portion marked 0,0, in Fig. 13, the amount of deformation was nil; that is, the thickness of the walls of the cones at these regions was the same as that of the original sheet. An increase in DPH was noted in this region of zero deformation of between 5 and 10 units.

Microstructure of the Formed Specimens. The microstructure of the "as received" sheet (2024-T4) was as shown in Fig. 15, and that of the annealed but unworked sheet (2024-0) was as shown in Fig. 16. The change of structure due to the annealing treatment was clearly noticeable. In the "as received" sheet, there appeared to be no precipitate of the compound Al_2Cu. This was natural because of the -T4 temper. The small dark-appearing

discrete particles, which were seen in all the photomicrographs at all stages of forming and cold rolling, appear to be the insoluble compounds, (Mg-Si) and (Al-Cu-Fe-Mn) (4). In the annealed sheets the compound Al_2Cu had precipitated preferentially along the grain boundaries and can be seen as a network of light colored bands (Fig. 16). Photomicrograph shown in Fig. 17 was that obtained from a formed specimen at a portion deformed approximately 25%. The elongation and preferred orientation of the grains can be clearly seen on comparing with Fig. 16. At portions of greater deformation, more preferred orientation and crystallographic fibering and some grain fragmentation were noticed. The photomicrograph, Fig. 18, was typical of the microstructure at the region of the apex of the cones. It was also noticed that with greater amounts of deformation (approximately greater than 50%) the clearly distinguishable network of thin black lines denoting the separate grains (visible in Figs. 16 and 17) were not visible at all. For example, these lines are not visible in Fig. 18. The different grains could be detected only by the network of light colored bands formed by the precipitation of Al_2Cu during annealing. However, it was apparent that there was no change, so far as the microconstituents or microphases were concerned, due to the explosive forming.

Hardness. The DPH of the 2024-O (annealed) unformed sheet was 58.4. The DPH of the conical portion studied (positions 1 to 23, Fig. 13) varied from a minimum of 66 units (position 2, Table 2) to a maximum of 96.5 units (position 7, Table 5). Thus the entire formed piece had a DPH greater than that of the parent

material of between 7.6 and 38.1 units.

The overall hardness pattern of the longitudinal section of the cone was somewhat different from that obtained by Tardif (compare Fig. 25 with Fig. 1). However, in the region of the apex, the hardness pattern obtained (Fig. 25) was similar to that obtained by Tardif; that is, in the region of the apex, there was an increase in hardness over that of the adjacent portions of 5 to 7 units.

Deformation. The thickness of the parent sheet was 0.051 inch, and the wall thickness of the conical portion studied varied between a minimum of 0.018 inch (position 12, Table 3) at the apex region to a maximum of 0.041 inch at the base of the conical portion (position 1, Tables 3 and 6). Some portions at the flange (wrinkled) had a maximum thickness of 0.054 inch, but this portion was neglected for reasons mentioned heretofore.

There appeared to be no consistent relationship between the amount of deformation per cent and the concomitant increase in DPH per cent. The graph (Fig. 26) relating these two showed much scatter and overlap. Therefore, it appeared to be useless for predicting the hardness increase per cent for a given deformation per cent even within its range of values.

Cold Rolled Samples

Microstructure. The microstructure of the parent metal was as shown in Fig. 15. Figure 21 was the photomicrograph of a specimen cold rolled to a thickness of 0.029 inch, that is, deformed 43.2%. The preferred orientation and crystallographic

Table 7. The position, individual DPH numbers obtained for each sample tested, and the average values of DPH are shown.

Position on sample	Sample 1 DPH	Sample 2 DPH	Sample 3 DPH	Sample 4 DPH	Sample 5 DPH	Average DPH	Increase in DPH (average)	Per cent increase in DPH (average)
1	73.9	76.6	75.3	80.2	79.5	77.1	18.7	32.1
2	66.0	67.7	66.6	71.3	69.5	68.2	9.8	16.8
3	68.9	70.1	71.3	74.6	72.6	71.5	13.1	22.4
4	72.6	73.9	75.3	78.8	76.6	75.4	17.0	29.2
5	76.6	78.0	79.5	82.5	81.0	79.5	21.1	36.2
6	81.8	83.3	84.1	87.4	86.6	84.6	26.2	45.0
7	90.0	91.8	92.7	96.5	94.6	93.1	34.7	59.5
8	87.4	88.3	89.1	93.7	91.8	90.1	31.7	54.4
9	83.3	84.9	85.7	90.0	87.4	86.3	27.9	47.8
10	81.8	82.5	83.3	87.4	85.7	84.1	25.7	44.1
11	76.6	78.0	78.8	82.5	81.8	79.5	21.1	36.2
12	82.5	83.3	84.1	89.1	86.6	85.1	26.7	45.8
13	75.3	76.6	77.3	81.0	80.2	78.1	19.7	33.8
14	78.0	80.2	81.0	84.1	83.3	81.3	22.9	39.2
15	84.1	86.6	87.4	89.1	90.0	87.4	29.0	49.7
16	86.6	89.1	90.9	92.7	91.8	90.2	31.8	54.5
17	89.1	90.9	92.7	95.6	94.6	92.6	34.2	58.6
18	80.2	84.1	84.1	85.7	86.6	84.1	25.7	44.1
19	75.9	78.8	78.8	81.0	82.5	79.4	21.0	36.0
20	73.9	75.9	76.6	79.5	80.2	77.2	18.8	32.2
21	67.2	69.5	70.1	73.3	72.6	70.5	12.1	20.7
22	66.6	68.9	69.5	72.6	72.0	69.9	11.5	19.7
23	78.0	75.3	74.6	82.5	81.8	78.4	20.0	34.2

Table 8. The position, thickness obtained at each position of each of the five samples tested, and the average thickness and the deformation per cent at each position are shown.

Position on cone	Sample 1: Thickness, inches	Sample 2: Thickness, inches	Sample 3: Thickness, inches	Sample 4: Thickness, inches	Sample 5: Thickness, inches	Average thickness, inches	Decrease in thickness (average), inches	Per cent decrease in thickness (average)
1	0.040	.041	.039	.038	.041	.040	0.011	21.6
2	0.038	.039	.038	.038	.040	.039	0.012	23.5
3	0.036	.038	.034	.037	.038	.037	0.014	27.4
4	0.035	.035	.034	.034	.037	.035	0.016	31.4
5	0.033	.034	.033	.032	.035	.035	0.016	31.4
6	0.031	.031	.033	.032	.033	.032	0.019	37.2
7	0.031	.030	.032	.030	.032	.031	0.020	39.2
8	0.030	.028	.029	.030	.031	.030	0.021	41.1
9	0.028	.028	.026	.027	.027	.027	0.024	47.0
10	0.026	.025	.025	.024	.024	.025	0.026	51.0
11	0.022	.021	.020	.021	.020	.021	0.030	58.8
12	0.020	.018	.019	.019	.019	.019	0.032	62.7
13	0.020	.020	.021	.022	.018	.020	0.031	60.7
14	0.021	.022	.021	.022	.020	.021	0.030	58.8
15	0.024	.026	.024	.025	.023	.024	0.027	53.0
16	0.028	.029	.028	.027	.028	.028	0.023	45.1
17	0.029	.029	.029	.030	.030	.029	0.022	43.1
18	0.030	.031	.030	.030	.031	.030	0.021	41.1
19	0.032	.033	.033	.032	.033	.033	0.018	35.3
20	0.033	.034	.035	.035	.033	.034	0.017	33.3
21	0.036	.037	.037	.038	.036	.037	0.014	27.4
22	0.038	.039	.038	.038	.037	.038	0.013	25.5
23	0.039	.040	.041	.039	.038	.039	0.012	23.5

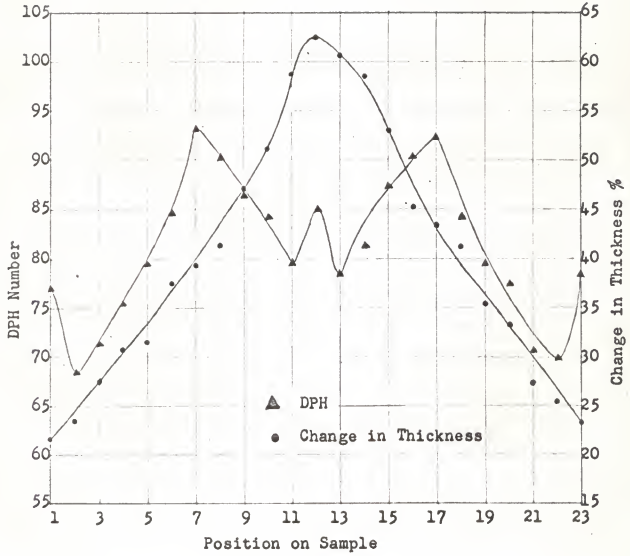

Fig. 25. Graphs of DPH number versus position on sample, and change in thickness per cent versus position on sample (compare with Fig. 1), obtained for the explosively formed specimens.

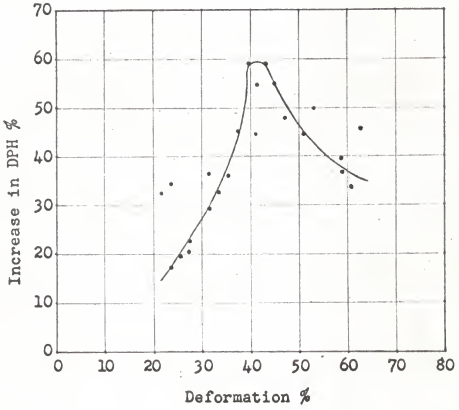

Fig. 26. Effect of deformation on the DPH of explosively formed 2024-O aluminum alloy.

fibering of the grains were well apparent, just as in the case of explosively formed pieces. Figure 22 was the photomicrograph of a sample cold rolled to a thickness of 0.011 inch; that is, deformed 78.5%. The extreme fragmentation of the grains was noticeable. In fact, in this photomicrograph, it was difficult to distinguish the separate grains.

However, there was apparently no change in the microconstituents or microphases.

Microhardness (DPH) and Deformation. The samples were deformed by various amounts to a maximum of 78.5%. The hardness always increased with increasing amounts of deformation. The rate of increase of hardness per cent with the amount of deformation per cent (Fig. 27) was at first quite rapid; but at greater amounts of deformation, the rate of increase of hardness tended to decrease. The graph relating the per cent deformation and per cent increase of hardness appeared to be quite useful for predicting the approximate hardness of a sample, when it was deformed by an amount within the range of the graph.

Deforming the 2024-O sheet to an extent greater than about 70% tended to produce cracks on the deformed sample which were normal to the direction of rolling.

Table 9. The thickness and DPH of 2024-0 Alclad aluminum alloy sheet, originally 0.051 inch thick, cold rolled by various amounts.

Trial No.	Thickness, inches	% decrease in thickness	Mean diagonal, mm.	DPH	Increase in DPH	% Increase in DPH
-	0.051	0.0	0.0252	58.4	0.0	0.0
1	0.048	5.9	0.0222	75.3	16.9	29.0
2	0.044	13.7	0.0218	78.0	19.5	33.4
3	0.041	19.6	0.0216	79.5	21.1	36.2
4	0.037	27.4	0.0210	84.1	25.7	44.1
5	0.033	35.2	0.0204	89.1	30.7	52.5
6	0.031	39.2	0.0200	92.7	34.3	58.8
7	0.029	43.2	0.0197	95.6	37.2	63.6
8	0.024	53.0	0.0193	99.6	41.2	70.5
9	0.019	62.7	0.0191	101.7	43.3	74.2
10	0.011	78.5	0.0188	104.9	46.5	79.6

DISCUSSION

Initially, attempts were made to form the workpieces using pelletless shotgun shells as the energy source; that is, the forming was sought to be done by gas pressure only. Those attempts were unsuccessful due to various probable causes, some of which might have been the following: (a) Commercial smokeless powders are manufactured so as to satisfy certain stringent service requirements. The powders do not function satisfactorily, if the service conditions are different from those intended. The most important of these service conditions are the sectional density of the bullet and the borecase volume (1). Evidently, these were unsuitable in our research equipment. (b) Smokeless powders deflagrate more efficiently when the pressures are raised; that is, the deflagration depends directly on

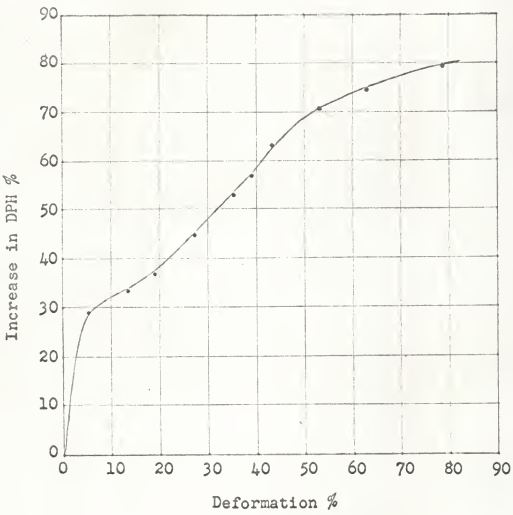

Fig. 27. Effect of deformation on the DPH of cold worked 2024-0 aluminum alloy.

the degree of confinement of the gases. Again, in our equipment, the degree of confinement of the gases, without the loading of lead shot, appears to have been insufficient to cause the powder charge to burn completely and, hence, resulted in unburned powder and insufficient pressures.

If black gun powder had been used instead of smokeless powders, perhaps the results would have been better, as black gun powder has a more rapid burning characteristic than smokeless powders at lower pressures and, hence, would by itself pressurize the system (10).

Black powder, however, was not used as it is a greater safety hazard than smokeless powders, it would excessively dirty the equipment after each shot, and it would ruin the equipment after some shots by chemical action, as it contains sulfur.

Water was not useful as a transfer and attenuating medium, as the gas pressure attained was insufficient.

"Hercules Red Dot" powder, being a more rapid burning powder than the other types tried, gave more satisfactory results. This was because the barrel length of the apparatus was approximately seven inches compared to about twenty-six inches for commercial barrels. Therefore, it was natural for the more rapid burning powder to give better results in the short barrel.

All the "shots" were fired with all the four spacers in position, since the removal of the spacers would further shorten the barrel and, in turn, decrease the deflagration of the powder charge. Moreover, the removal of one or more spacers would have increased appreciably the time consumed for tightening the

fifteen nuts on the cover plate.

The formed pieces were highly wrinkled at their base or flange portion. This was probably because the forming member (the buffer) was much smaller at its contact area with the workpiece than the die cavity opening, and this difference caused the wrinkling at the open end of the cone and the apparent "metal gathering" or increase of thickness.

Tardif used high explosives combined with a transfer medium, such as water, for his forming process. High explosives, when so used, produce reflected shock and pressure waves at the interface of the explosive and transfer medium and the interface at the surface of the container (3). Conceivably, the metal gathering obtained by Tardif was due to the above phenomenon of reflected waves. In the method of forming tried in this research, there appeared to be little probability of reflected waves. More probably, the thickening was due to the wrinkling prevalent at this portion of the formed pieces. The small amount of thickening (6% in our case compared to 32% obtained by Tardif) seemed to confirm this conjecture. Similarly, the small increase in hardness of about 4-10 units noted in this region was possibly due to the bending and wrinkling prevailing in this region.

The apexes of the formed cones had a rough grainy appearance and were rounded to a diameter of approximately one inch. The grainy appearance and rounding were probably due to the fact that the formed piece took the shape of the forming member (buffer). As the buffer was flat at its contact surface with the workpiece, this bluntness was more or less reproduced on the

formed piece. The surface at the apex was grainy, as this portion was probably not in contact with the die surface during the forming cycle, unlike the straight portions of the cones, because the cones were not formed to the full depth of the die cavity; also, the portion near the apex, being the first to come in contact with the forming member and because of the rapidity of the forming cycle, appears to have been overstretched, giving rise to the rough grainy appearance. Probably, if a buffer of more suitable shape were to be used (the shape has to be developed experimentally), the cones would be formed deeper and less blunt and with less wrinkling at the base and less roughness at the apex. The wrinkling may also be minimized, if the die cavity were better designed, or if a workpiece of a somewhat smaller diameter were used.

The time consumed for each shot was about one hour. The time factor alone, even if the formed piece were perfect, would preclude the use of this method being adapted for production purposes.

The maximum depth of the cones formed, without cracking, was one and three-sixteenths inch. Greater depths could be obtained in press machinery, though perhaps not in a single drawing operation or without intermediate annealing. The wall thickness of the cones varied from a maximum near the base to a minimum near the apex; this non-uniform wall thickness is not desirable in deep drawing operations. Therefore, it was concluded that the equipment and the method were not the most suitable for deep drawing aluminum alloys.

Preferred orientation, grain elongation, and crystallographic fibering were observed after both methods of deformation. This was quite usual and expected in all ductile materials which were worked when "cold". No changes in the microphases were detected. The solidus temperature for 2024 type aluminum alloy is 935°F., and the recrystallization temperature at approximately 50 per cent deformation is 650°F. As no evidence of recrystallization was noticed anywhere in the formed pieces, it can be stated that the forming took place entirely in the "cold" condition. Even if the temperature had reached the recrystallization temperature during forming, the time at temperature would have been insufficient to cause any structural (phase) change in the alloy, as the forming operation took place in fractions of a second.

The thin dark lines at the grain boundaries, visible in Figs. 16, 17, and 21, are not visible in Figs. 18 and 22 which show the microstructure at greater deformations, indicating that the grains have been compressed together laterally while being elongated longitudinally, thus obliterating these grain boundary lines. The insoluble (Mg-Si) and (Al-Cu-Fe-Mn) compounds, which appear as small dark discrete particles in all the photomicrographs, do not appear to have suffered any appreciable elongation or fragmentation due to the forming or rolling, showing perhaps, that they were much harder than the matrix material.

The hardness pattern obtained for 2024-O aluminum alloy cones (Fig. 25) was of a different shape than that obtained by Tardif (Fig. 1). In this research, the maximum hardness was

attained in the region of approximately 40-45% deformation (reduction), compared to approximately 20-25% deformation (increase in thickness) obtained by Tardif. This was, probably, because of the difference in forming methods and materials.

The hardness values (or increase in hardness) obtained by both methods of deformation (explosive forming and cold rolling) appear to be approximately equal until about 40% decrease in thickness of the sheet metal. Beyond 40% deformation, the graph of increase in hardness per cent versus decrease in thickness (deformation) per cent (Fig. 27) obtained for cold rolling continued to rise for increase in deformation. In the case of explosively formed sheet, the values of hardness began to fall after about 40% deformation (Fig. 26). Thus, there was no consistent relationship between the increase in hardness and the extent of deformation in the case of the explosively formed pieces, as was observed in the case of the cold rolled pieces. The probable reason seemed to be that during explosive forming, the rubber buffer which acted as the forming member was itself deformed, unlike the steel rolls used for cold rolling.

Between positions 7 and 17 a fall of DPH was noticed (Fig. 25), even though the amount of deformation was greatest in this portion (40-62%). This portion was the blunt or rounded portion at the apex of the cones. The probable reason for the fall of hardness (even though the deformation was greater) may be the following: The straight portion or sides of the cone (where the hardness versus deformation values are approximately similar to the hardness versus deformation values obtained by cold

rolling) were compressed between the die surface and the buffer in addition to being drawn. Thus the forming action was similar to that in cold rolling; but the rounded or apex portion (where the hardness values are lower in spite of greater deformation) was only deep drawn and not compressed.

The abnormal increase in hardness at position 12 (Fig. 25), over that of the adjacent positions 11 and 13, was also obtained by Tardif. In this research, the reason for the above phenomenon may be the following: Immediately after the forming impact, the rubber buffers would rebound from the die and formed piece. The formed piece also would experience an elastic springback which may cause a secondary plastic deformation accounting for the increased hardness. However, it was unclear why this phenomenon should have taken place only at the apex. The abnormal increase in hardness may also be partly due to the maximum deformation at this position.

CONCLUSIONS

1. The principle of a recessed die without a blank holder can be used for explosively forming aluminum alloys.

2. The equipment and method used were unsuitable for deep drawing if the time consumed per "shot", the depth of forming, and the amount of wrinkling of the formed part were taken into account.

3. Pelletless shotgun shells did not produce the gas pressure needed for the forming operation.

4. The effects on the microstructure of the alloy due to

explosive forming and cold working were similar and resulted in grain elongation, crystallographic fibering, and grain fragmentation.

5. The increase in hardness, in relation to the amount of deformation during explosive forming, appeared to be erratic and inconsistent; whereas in the case of cold working, the values appeared to be consistent.

ACKNOWLEDGMENTS

The author hereby expresses his thanks and gratitude to Dr. A. E. Hostetter, major adviser, for his guidance and encouragement; to Prof. C. L. Woodard, for his continuous and patient help and counsel during all stages of this research; and to Mr. C. L. Nelson, Instructor, Engineering Shops, for his assistance during the machining and photographing of the equipment.

BIBLIOGRAPHY

1. Amber, John T.
   Handloader's digest. 1st annual ed., Chicago: Gun Digest, 1962.

2. Dickinson, T. A.
   Behavior of metals under high-energy loads. The Tool Engineer 40(3):119-122. March, 1958.

3. Fedderson, E. W., and A. H. Peterson.
   High energy rate metal forming. Cleveland: American Society for Metals, n.d.

4. Fink, W. L., et al.
   Physical metallurgy of aluminum alloys. Cleveland: American Society for Metals, 1949. p. 111.

5. Ida, N. N.
   Explosive formability: four ways to improve it. Materials in Design Engineering 50(2):67-69. February, 1963.

6. Kehl, G. L.
   The principles of metallographic laboratory practice. New York: McGraw-Hill, 1949.

7. Peters, R. W.
   Impact and high-velocity forming. The Tool Engineer 39(1):83-86. July, 1957.

8. Pipher, F. C., G. N. Rardin, and W. L. Richter.
   High energy rate metal forming. United States Department of Commerce, Office of Technical Services AMC Technical Report 60-7-588. Washington: Government Printing Office, 1960.

9. Tardif, H. P.
   Techniques for explosive forming--forming cones by metal gathering. Metal Progress 76(3):84-85. September, 1959.

10. Taylor, J.
    Solid Propellent and exothermic compositions. New York: Interscience Publishers, 1959.

11. Wick, C. H.
    Chipless machining. New York: Industrial Press, 1960.

12. Wolf, P. J.
    Superalloys formed with explosives. The Tool Engineer 41(6):78-82. December, 1958.

MICROSTRUCTURAL CHANGES IN EXPLOSIVELY FORMED 2024-O ALUMINUM ALLOY

by

C. VENKATESH PRAKASH

B. E., University of Mysore, 1957

AN ABSTRACT OF A MASTER'S THESIS

submitted in partial fulfillment of the

requirements for the degree

MASTER OF SCIENCE

Department of Industrial Engineering

KANSAS STATE UNIVERSITY
Manhattan, Kansas

1964

The purpose of the research was to determine whether 2024-O aluminum alloy could be formed, using a recessed die without a blank holder and employing smokeless gunpowder as the energy source. The hardness pattern along a midsection of the formed cones was to be studied, and this pattern was to be compared with the pattern obtained by Tardif. Changes in hardness and microstructure of the same alloy, deformed by explosive forming and cold rolling, were also to be compared.

Efforts at forming with pelletless shotgun shells having failed, a forming technique was developed, employing handloaded shotgun shells with pellets. Buffers had to be used to prevent the lead shot from perforating the workpieces and also to aid the forming operation. After consistent forming had been obtained, the walls of the formed cones were studied for per cent deformation, microstructure, and microhardness (DPH). The same alloy sheet was then deformed to various thicknesses by cold rolling and examined for any resultant changes in microstructure and hardness.

It was found that pelletless shotgun shells did not deliver sufficient pressure for the forming operation, and that the equipment and method employed were not suitable for production purposes. The overall hardness and deformation patterns obtained were different from those obtained by Tardif, except in the region of the apex. The effects on the microstructure were the same under both types of deformations. Above forty per cent deformation, however, the relationship between per cent deformation and hardness became inconsistent in the case of the explosively formed samples.